Dust deposition minimization on the solar PV panel by solid wind barrier: A CFD modeling

Saeed Siahchehrehghadikolaei[1], Goodarz Ahmadi[1*], Mohammad A. Moghimi[2]

[1]Department of Mechanical and Aerospace Engineering, Clarkson University, Potsdam, NY 13699 USA

[2]Department of Engineering, Staffordshire University, Stoke-On-Trent, UK

August 2-4, 2022

Outline

- Objectives

- Geometry of the problem, its dimensions, and location information
- Mesh generation and its sensitivity tests
- Governing equations
- Boundary conditions and methodology
- Validation
- Results and discussion:
  - Dust particles deposition on PV panels
  - Dust particles deposition on the ground,
  - Airflow velocity and TKE contours
  - Airflow traces, and dust particles trajectories
- The PV module efficiency reduction prediction
- Conclusions

Objectives

Evaluate the wind flow over a solar PV field and dust particles deposition on the PV panel in the presence of a solid wind barrier with a flap.

Optimize the barrier geometry to minimize dust deposition on the PV surfaces.

Summary

A numerical simulation of the airflow and dust particle transport and deposition in the presence of a wind barrier was performed for different wind speeds. Several barrier geometries are studied. The barrier that minimizes dust deposition on the PV surfaces are identified.

Geometry

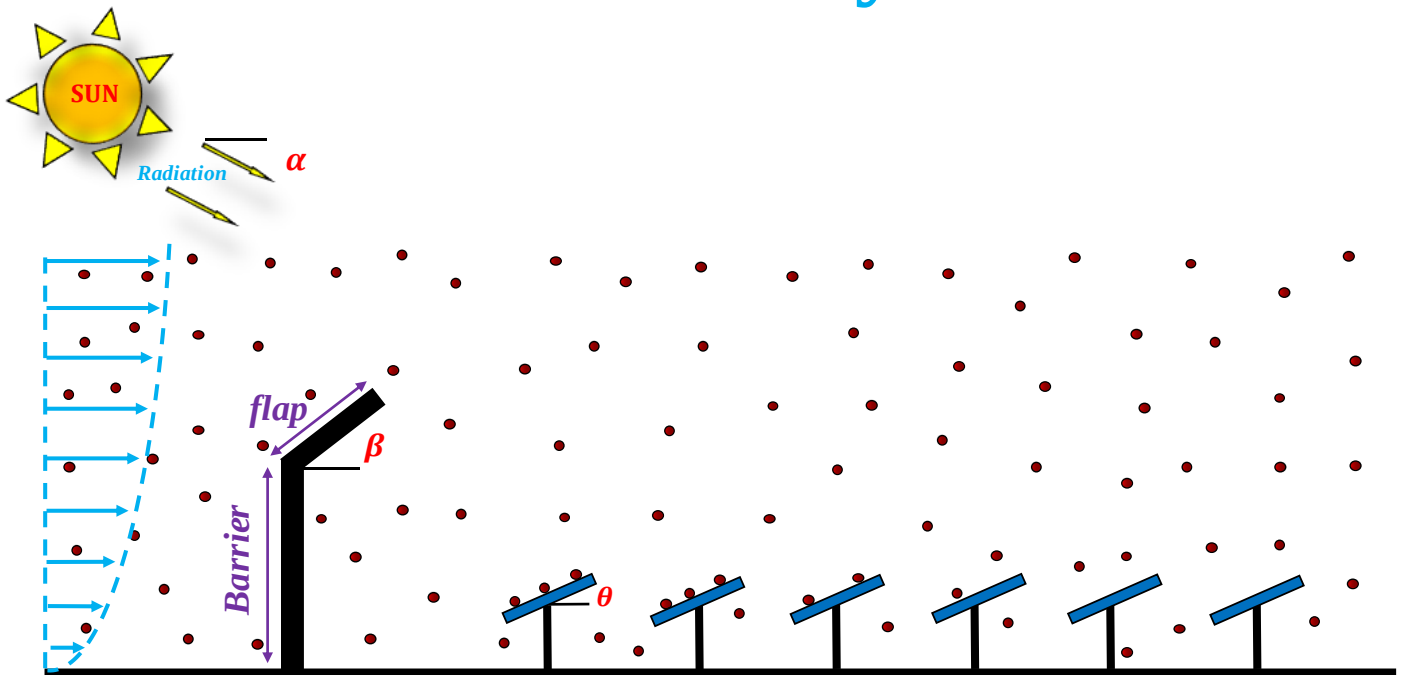

Fig.1. Schematics of the solar field with barrier. Location 37.8° N (San Francisco)

- **Barrier height (L4) (1,3.5 [m])**
- **Flap length (L5) (0.05, 0.5[m])**
- **Flap angle (β) (5, 175 [°])**
- **Dust particle size (dp) (50, 300[μm])**
- **Sand particles Density: ρ = 1350 [$kg.m^{-3}$]**

Dimensions

Table. 1 The dimensions of the geometry

Number of CASE	L4 (m)	L5 (m)	L6 (m)	β (degree)
CASE 1	2.38	0.30	5.51	90
CASE 2	3.73	0.50	7.58	174.21
CASE 3	3.73	0.49	8.09	6.74
CASE 4	3.72	0.11	7.61	8.28
CASE 5	1.01	0.10	2.41	167.62
CASE 6	1.09	0.49	3.12	6.93
CASE 7	1.01	0.49	2.62	164.39
CASE 8	3.70	0.12	7.47	171.69
CASE 9	1.11	0.11	2.71	10.77
CASE 10	2.37	0.10	5.08	129.63
CASE 11	2.97	0.50	7.04	85.59
CASE 12	1.74	0.30	3.81	172.45
CASE 13	3.71	0.30	8.08	50.44
CASE 14	2.46	0.22	5.37	7.91
CASE 15	1.00	0.34	3.08	67.61
CASE 16	3.14	0.31	6.44	174.47
CASE 17	2.42	0.41	5.59	11.94
CASE 18	2.36	0.49	5.09	169.14
CASE 19	3.57	0.12	7.40	90.01
CASE 20	1.07	0.15	2.77	89.11
CASE 21	1.64	0.48	4.46	94.02
CASE 22	2.09	0.12	4.63	59.41
CASE 23	3.73	0.40	8.15	118.38
CASE 24	1.41	0.30	3.47	5.44
CASE 25	1.04	0.28	2.85	126.43

$L1 = 100\ m;\ L2 = 20\ m; L3 = 12.5\ m; L7 = 1.3\ m;\ L8 = 3\ m; L9 = 5.84\ m;\ \alpha = 28\ °;\ \theta = 38\ °$

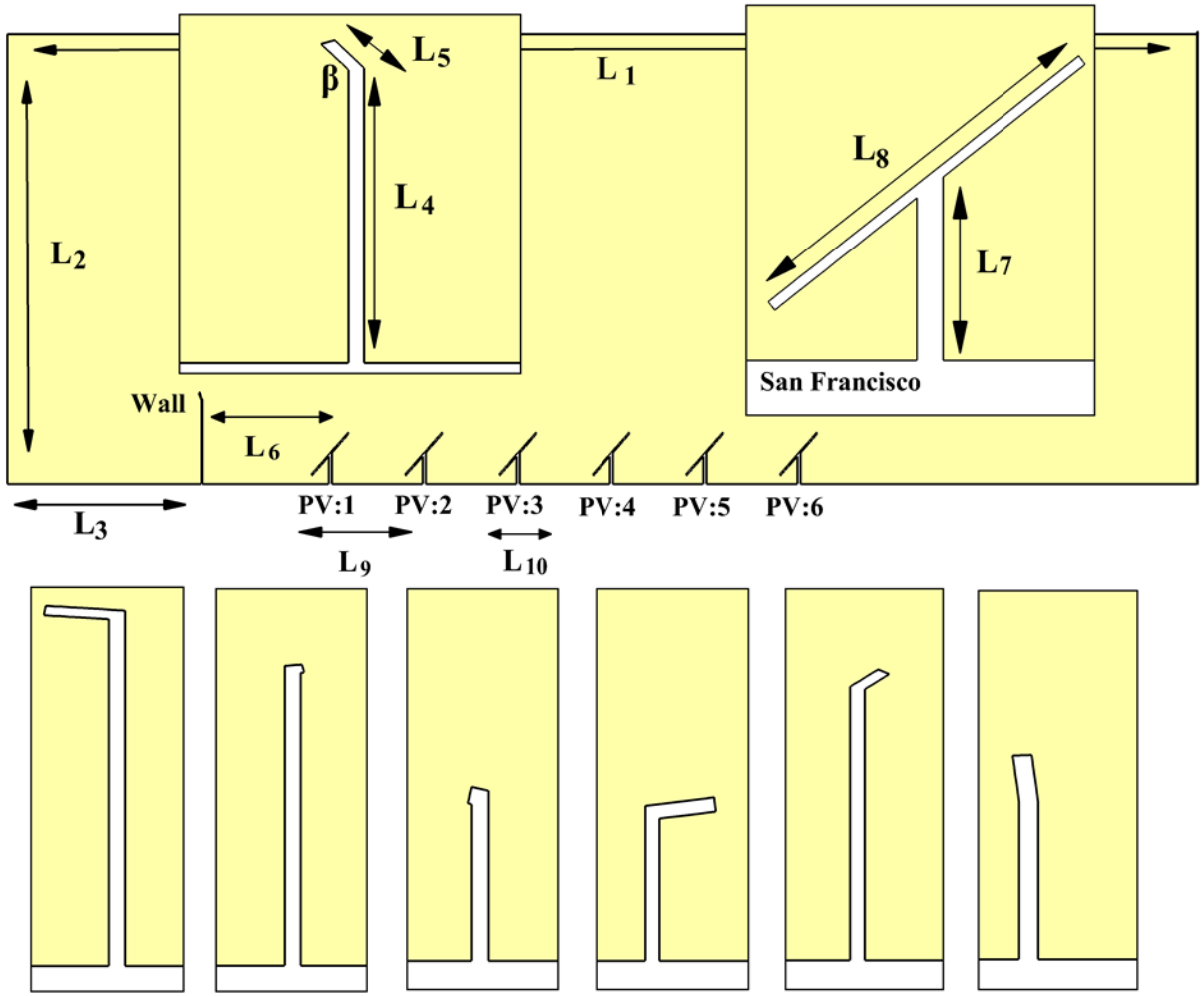

Fig.2. Different configurations of the wind barrier and its flap.

Grids generation

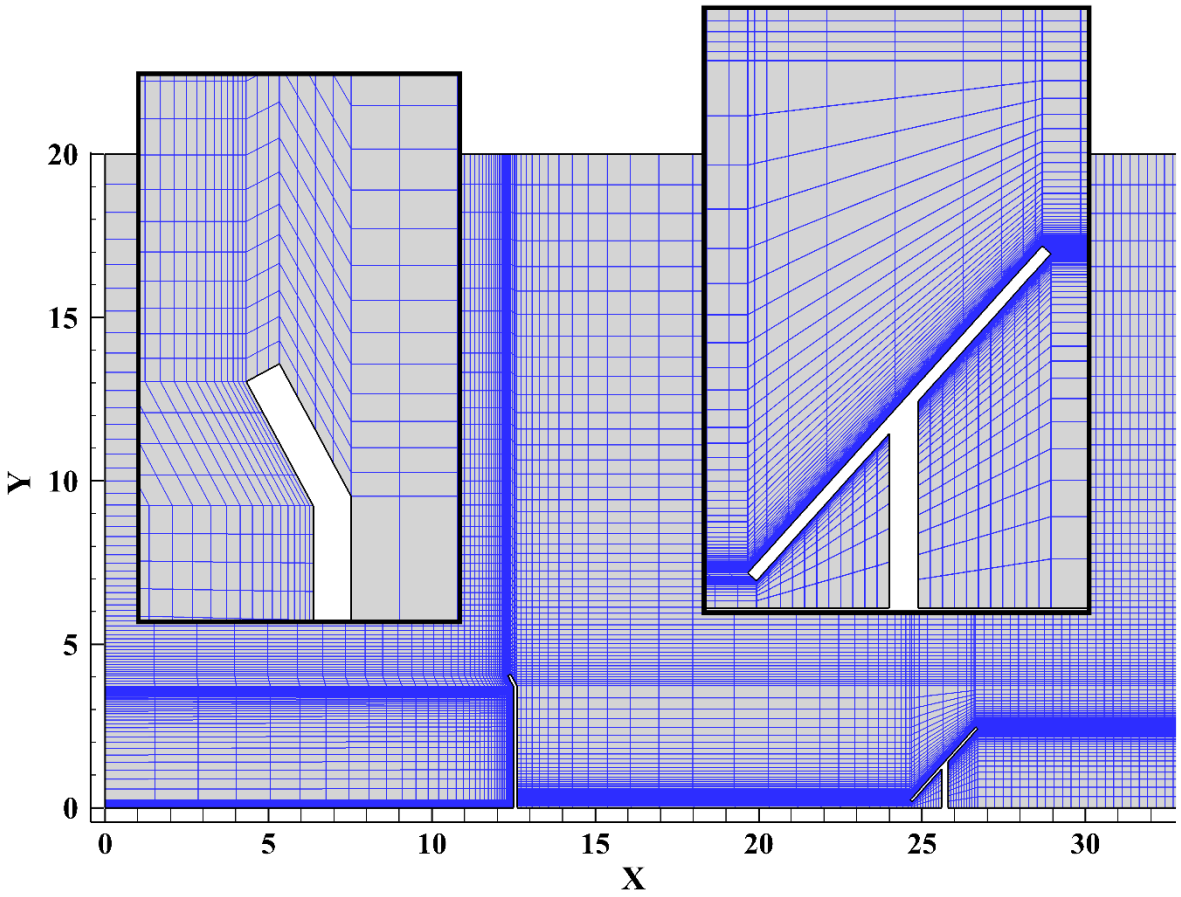

Fig.3. **Different configurations of the wind barrier and its flap.**

Table.2. **Grid sensitivity tests.**

Test specifications- CASE 23					
Mesh number	2.35×10^6	3.45×10^6	$\mathbf{4.55 \times 10^6}$	5.43×10^6	6.63×10^6
Dust deposition fraction %	5.23	4.83	**4.58**	4.62	4.60

Governing equations

Time-averaged mass and momentum equations for the turbulent air flow fields [1]

$$\frac{\partial \overline{u_i}}{\partial \overline{x}_i} = 0 \qquad (1)$$

$$\frac{\partial \overline{u_i}}{\partial t} + \overline{u_j}\frac{\partial \overline{u_i}}{\partial x_j} = -\frac{1}{\rho}\frac{\partial \overline{p}}{\partial x_i} + \frac{1}{\rho}\frac{\partial}{\partial x_j}\left(\mu\frac{\partial \overline{u_i}}{\partial x_j} - \rho\overline{u'_i u'_j}\right) \qquad (2)$$

Transport equations of the SST k-ω model [1]

$$\frac{\partial}{\partial t}(\rho k) + \frac{\partial}{\partial x_i}(\rho k u_i) = \frac{\partial}{\partial x_j}\left(\Gamma_k \frac{\partial k}{\partial x_j}\right) + G_k - Y_k + S_k \qquad (3)$$

$$\frac{\partial}{\partial t}(\rho \omega) + \frac{\partial}{\partial x_i}(\rho \omega u_i) = \frac{\partial}{\partial x_j}\left(\Gamma_\omega \frac{\partial \omega}{\partial x_j}\right) + G_\omega - Y_\omega + D_\omega + S_\omega \qquad (4)$$

[1] L. Tian, G. Ahmadi, (2007) Journal of Aerosol Science 38, 377-397.

Governing equations

Lagrangian equation of dust motions [2]

$$\frac{du_p}{dt} = \frac{1}{\tau}\frac{C_D Re_p}{24}\left(u_g - u_p\right) + \frac{g(\rho_p - \rho_g)}{\rho_p} + \xi\sqrt{\frac{\pi S_0}{\Delta t}} + \frac{2\rho K_c \nu^{0.5}}{\rho_p d_p (S_{lk}S_{kl})} s_{ij}\left(u - u_p\right) \qquad (5)$$

$$C_D = \begin{cases} \dfrac{24}{Re_p}, & Re_p < 1 \\ \dfrac{24}{Re_p}\left(1 + 0.15 Re_p^{0.687}\right), & 1 < Re_p < 400 \end{cases} \qquad (6)$$

[2] Z. Zhang, Q. Chen, Atmospheric Environment, 43 (2009) 319-328; https://doi.org/10.1016/j.atmosenv.2008.09.041

Boundary Conditions & Methodology

The wind velocity is 2.5 m/s or 3.86 m/s, and 5 m/s.
The outflow boundary condition was used in the outlet.
The no-slip boundary condition was employed for the walls.
The symmetry boundary condition was applied in the upper boundary.
The shear stress transport (SST)- K-ω turbulence model with User-Defined Function (UDF) inlet profiles used to predict turbulent airflow around solar PV panels.

Numerical settings (Ansys-Fluent)

-To break up the pressure from the velocity, the Semi-Implicit Method for Pressure Linked Equations (SIMPLE) is performed

- Pressure ~ Second order - Momentum ~ Second order - Turbulent Kinetic Energy ~ Second order

- Diameter Distribution ~ Rosin-Rammler method

-The dust particle motions in the computational domain and deposition on the PV surface are evaluated by the Discrete Phase Model (DPM)

Validation

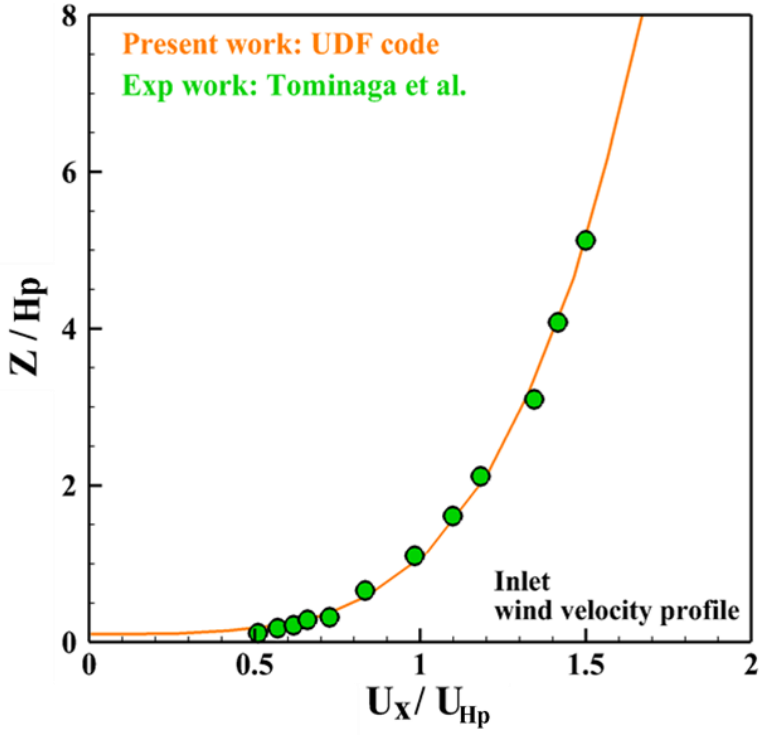

Fig. 4(a). Comparison of the inlet wind velocity profile.

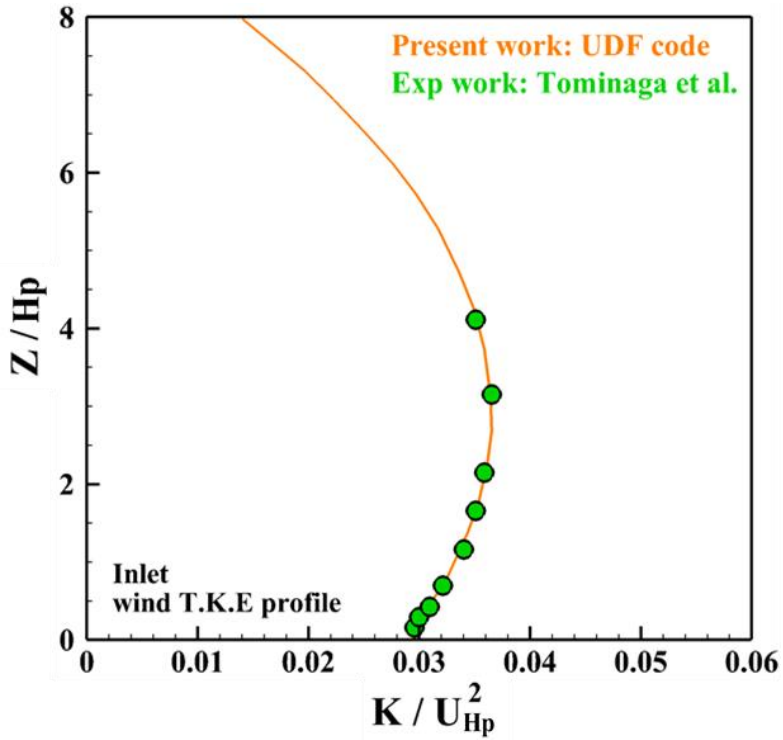

Fig. 4(b). Comparison the inlet TKE profile.

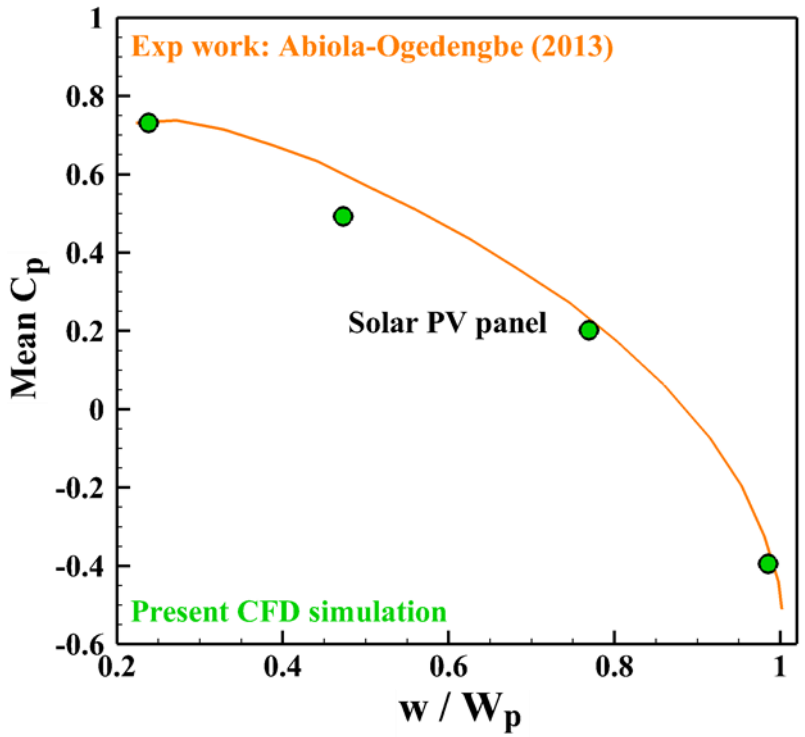

Fig. 4(c). Comparison the Mean Pressure along the upper surface of PV panel.

H_p: *Panel height (from the highest point to the ground)* U_{H_p}: *The air velocity at the PV height*; W_p: *Panel width (L8)*;
w: *The distance from the leading edge along the width of the solar PV panel*; U_X: *The mean velocity*

[3] Yoshihide Tominaga, Shin-ichi Akabayashi, Takuya Kitahara, Yuki Arinami, Building and Environment, 84 (2015) 204-213; https://doi.org/10.1016/j.buildenv.2014.11.012

[4] A. Abiola-Ogedengbe, University of Western Ontario-Electronic Thesis and Dissertation Repository, (2013) P1177

Dust deposition report

Wind velocity = 3.86 m/s

Number of released particles: 10,000,000

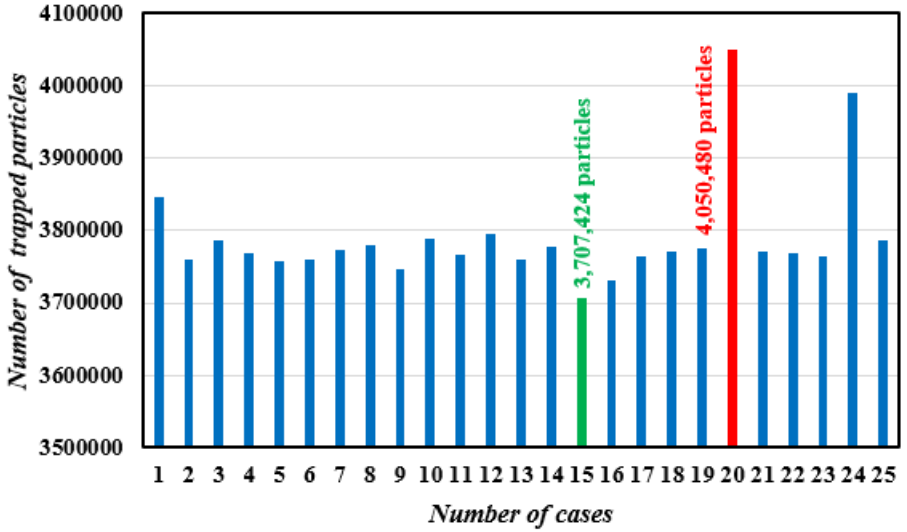

Fig. 5(a). Total number of trapped particles in the domain

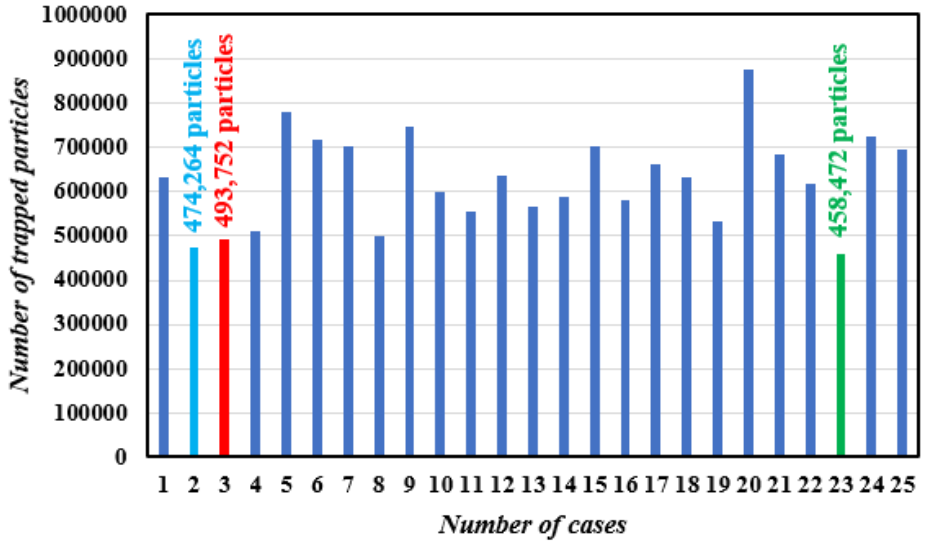

Fig. 5(b). Number of trapped particles on PV panels

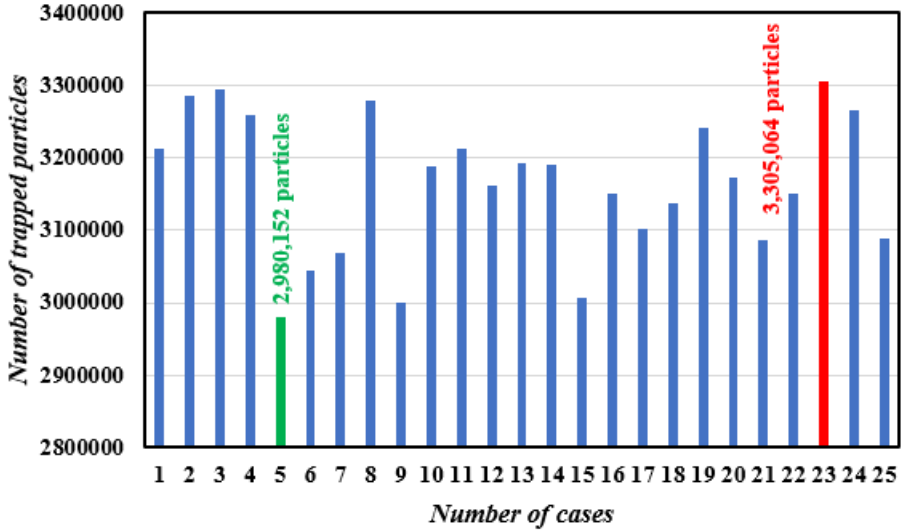

Fig. 5(c). Number of trapped particles on the ground

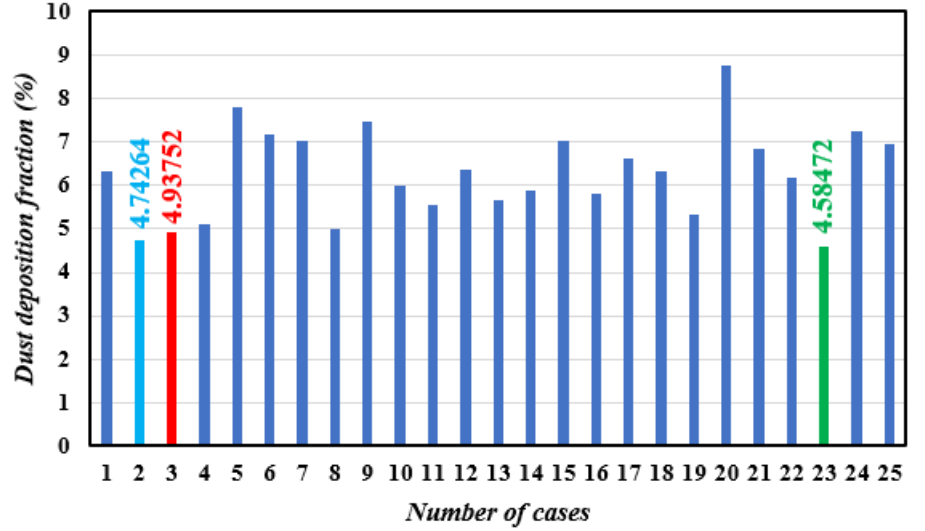

Fig. 5(d). Particle deposition fraction on PV Panels

Wind velocity = 3.86 m/s

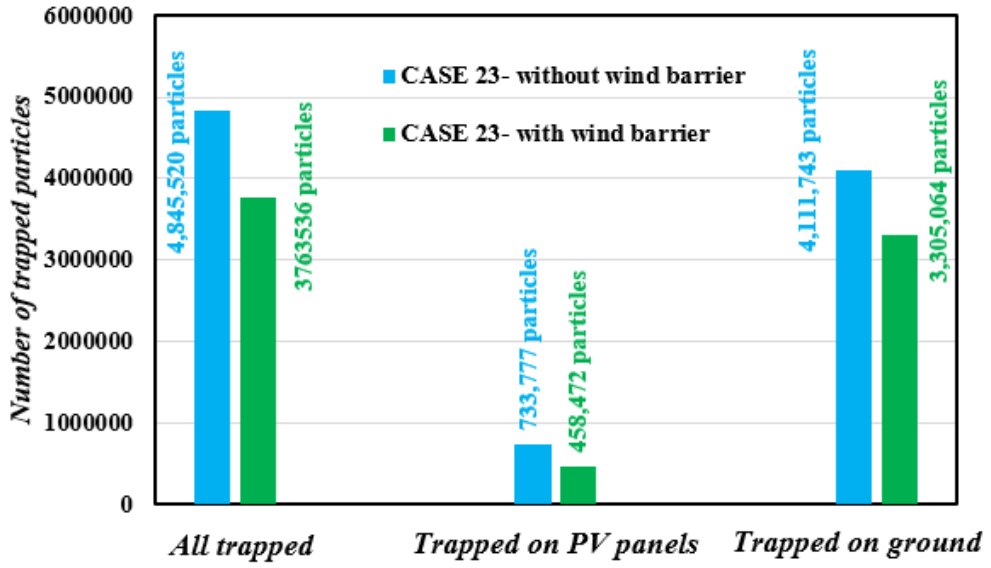

Fig. 5(e). Number of trapped particles on different regions

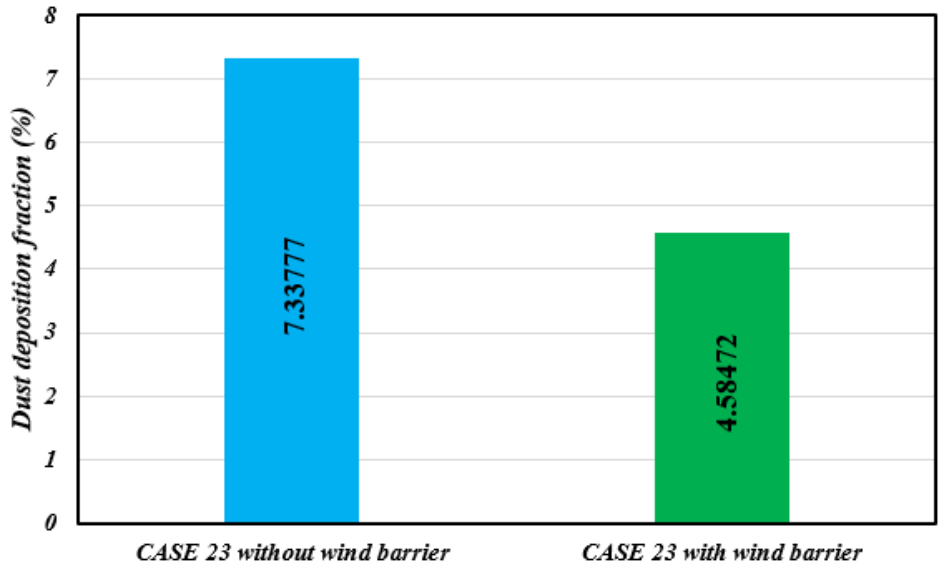

Fig. 5(f). Dust particles depostin fraction for CASE 23 with/without wind barrier

The dust deposition fraction [5]:

$$\lambda = \frac{N_d}{N_p} \times 100\%$$

N_d: *Number of deposited particles on PV panel*
N_p: *Numer of particles released at the inlet*

[5] Hao Lu, Wenjun Zhao, Renewable Energy, 131 (2019) 829-840; https://doi.org/10.1016/j.renene.2018.07.112

Velocity Contours

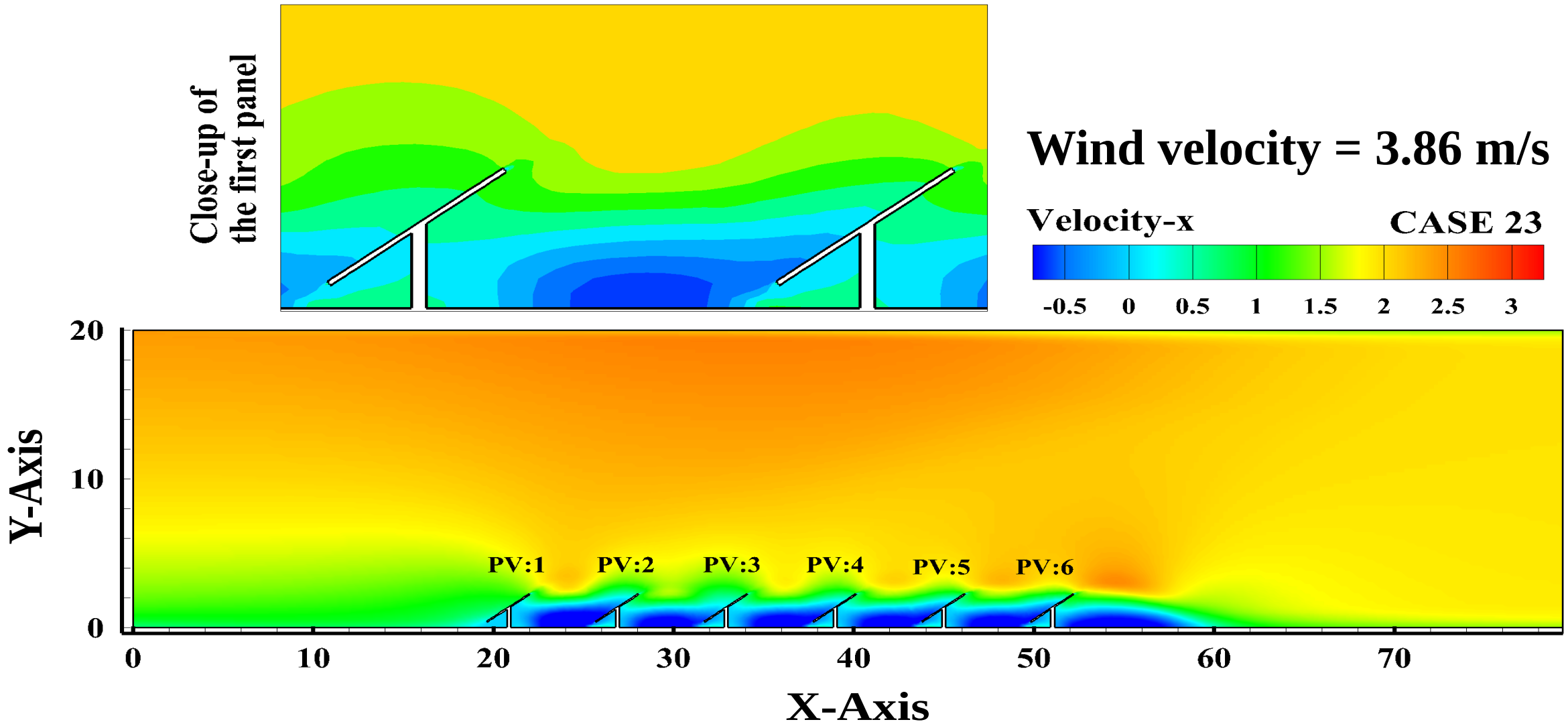

Fig. 6(a). **Velocity contours without wind barrier-CASE 23**

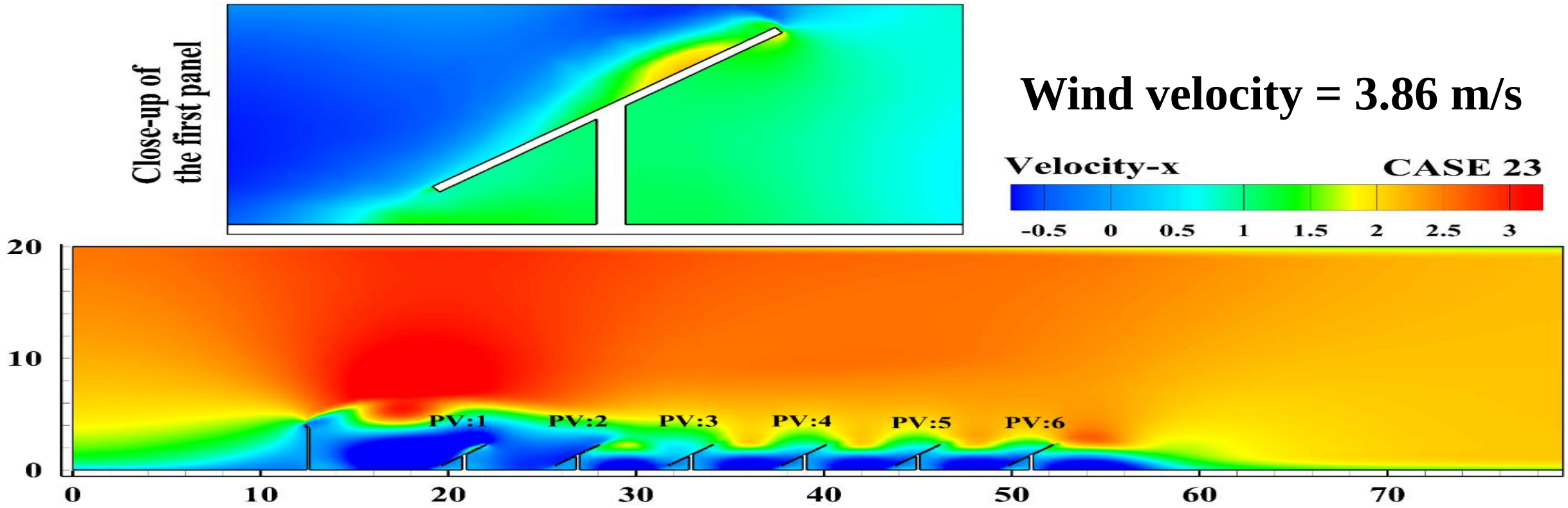

Fig. 6(b). **Velocity contours with wind barrier-CASE 23**

Turbulence Kinetic Energy Contours

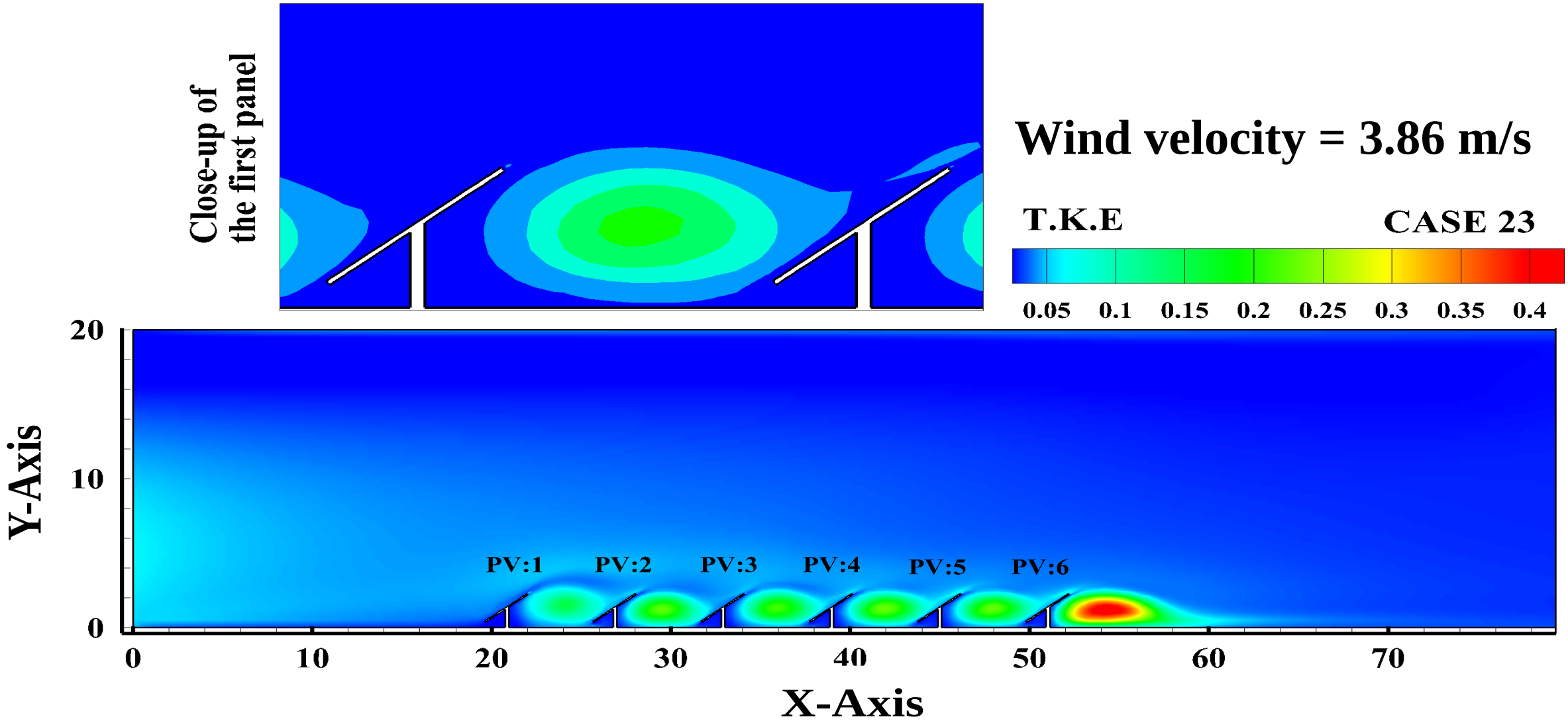

Fig. 6(c). TKE contours without wind barrier

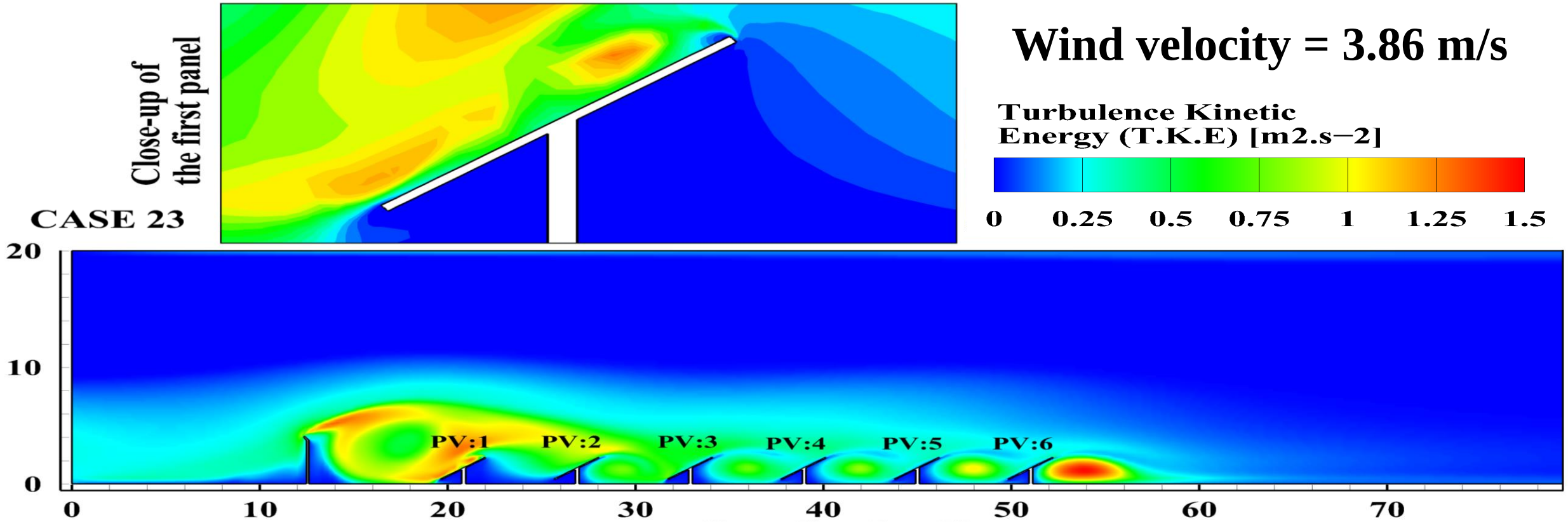

Fig. 6(d). **TKE contours with wind barrier- CASE 23**

Airflow traces

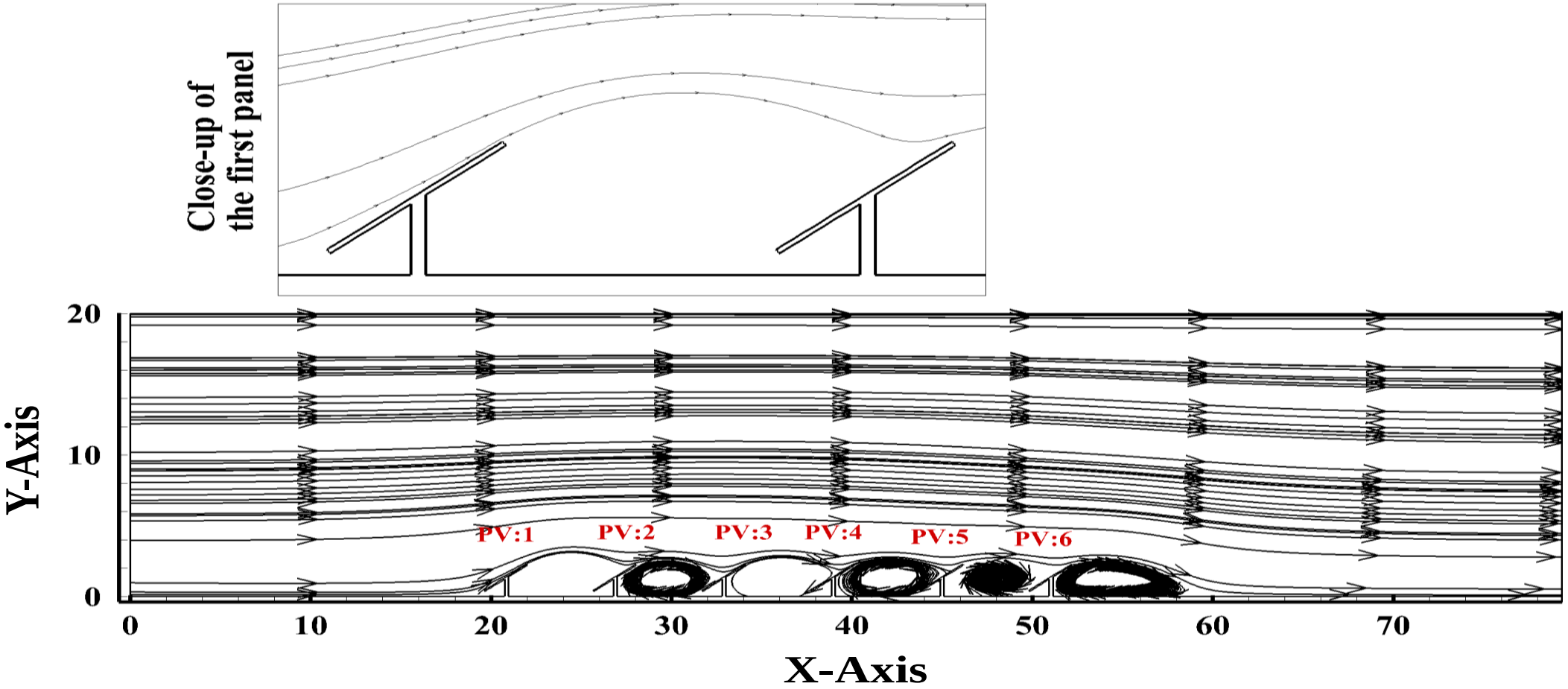

Fig.7(a). Different views of airflow traces - without wind barrier

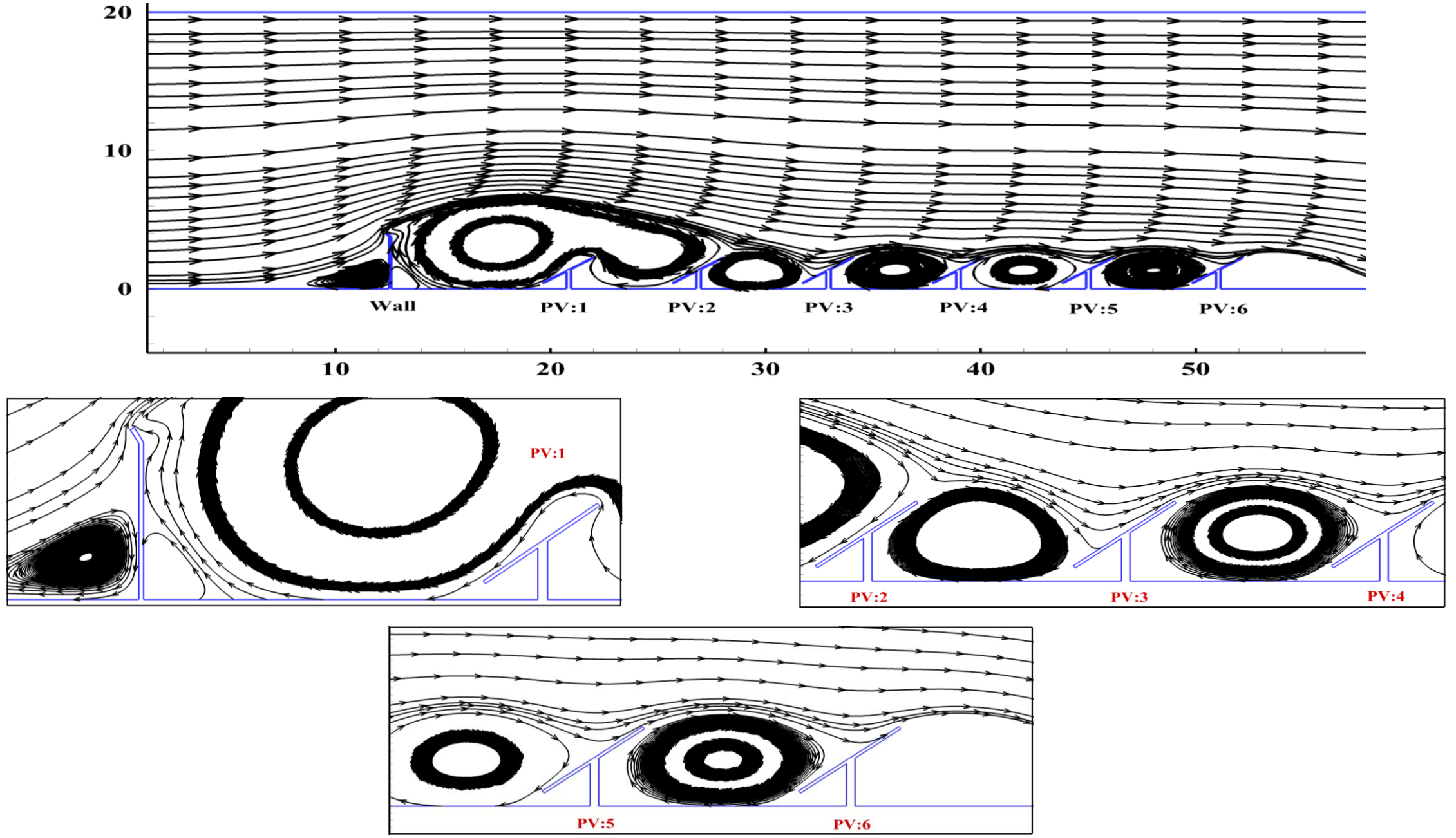

Fig.7(b). Different views of airflow traces - CASE 23 with wind barrier

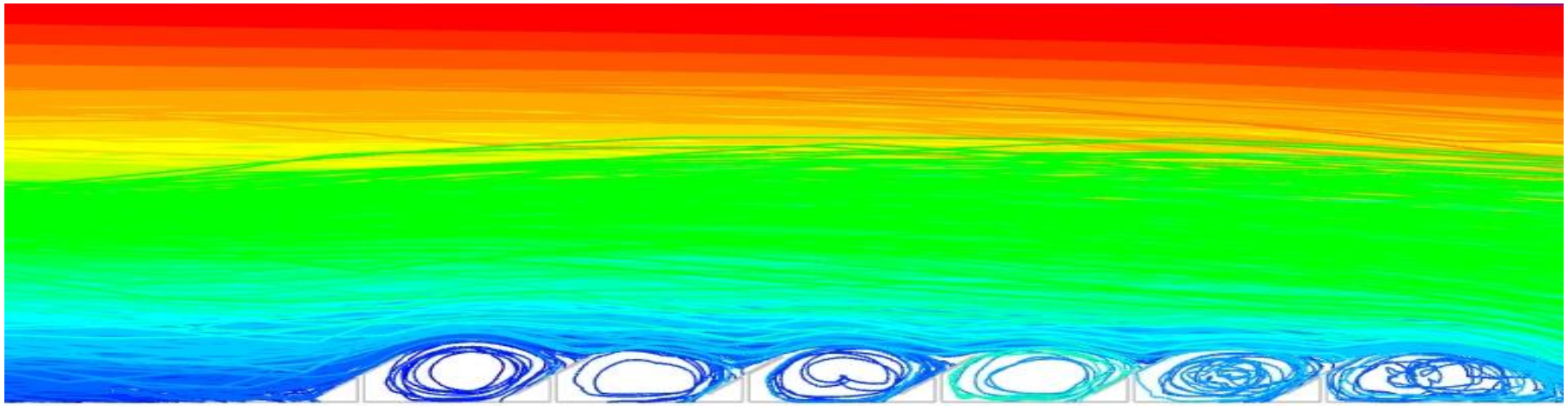

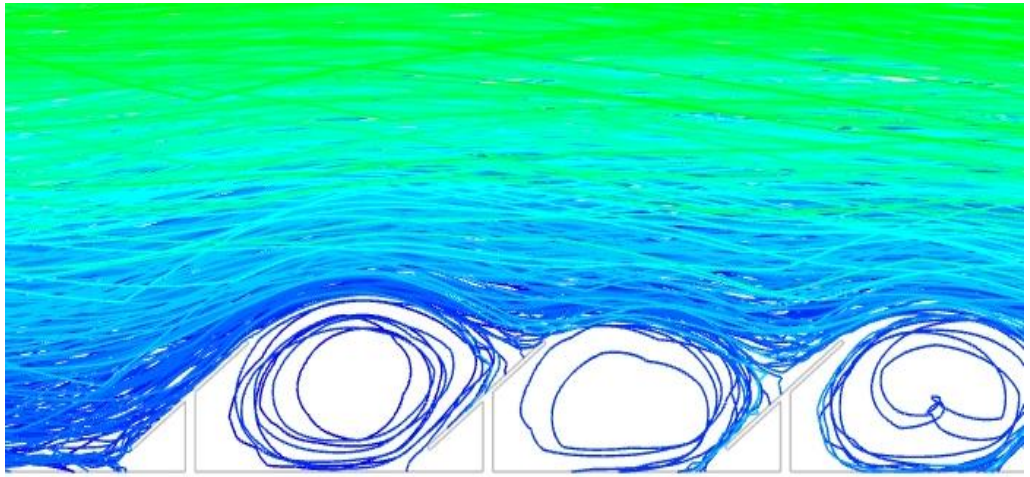

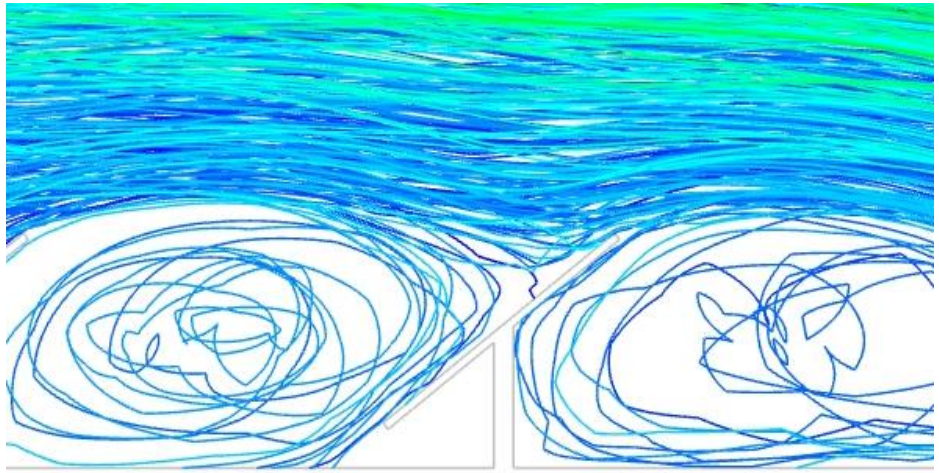

Fig.8(a). Different views of particles trajectory- without wind barrier; $U = 3.86 \frac{m}{s}, d_p = 50\ \mu m$

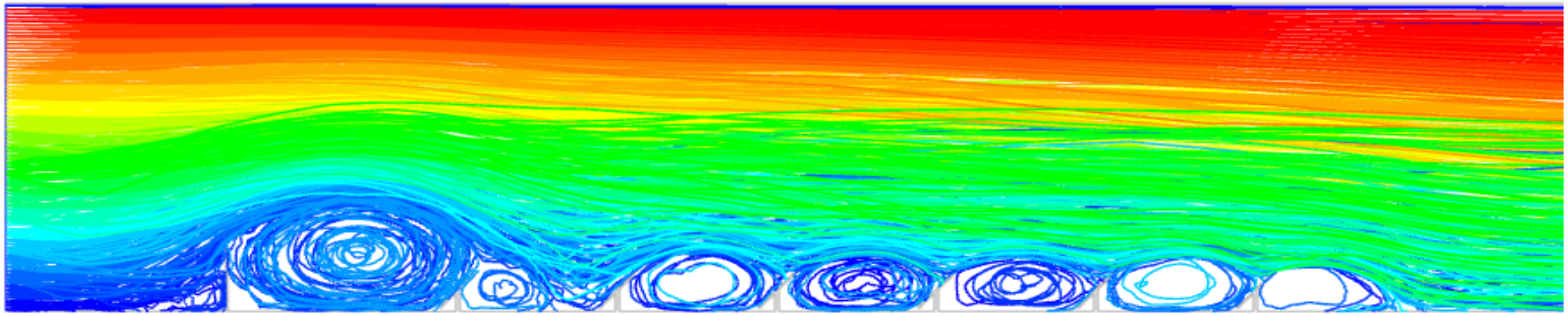

a) **Entire domain**

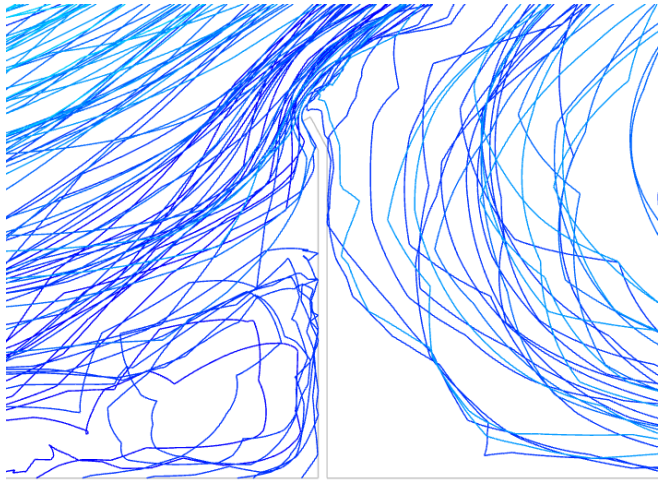

b) **Barrier and flap**

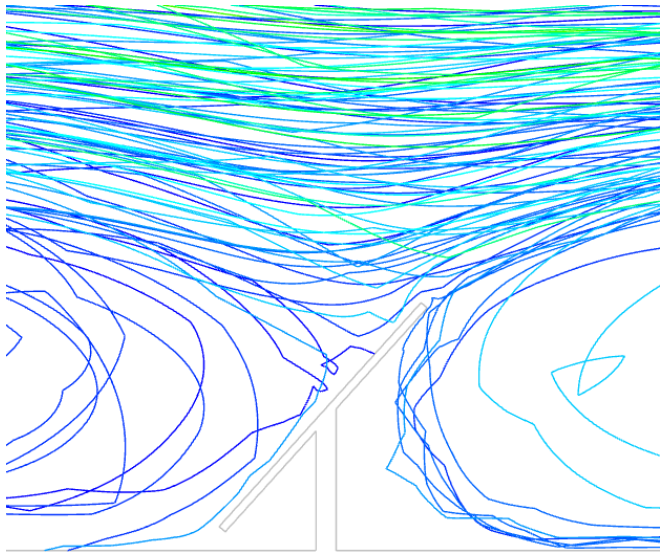

c) **Panel 1**

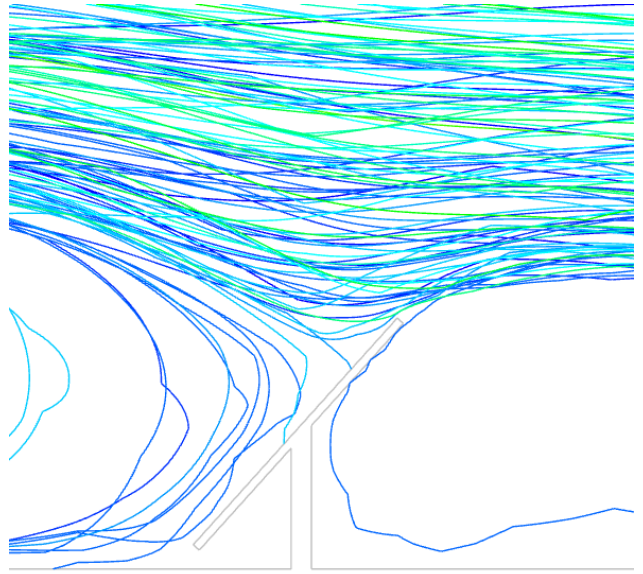

d) **Panel 6**

Fig.8(b). **Different views of particles trajectory- CASE 23 with wind barrier; $U = 3.86 \frac{m}{s}, d_p = 50\ \mu m$**

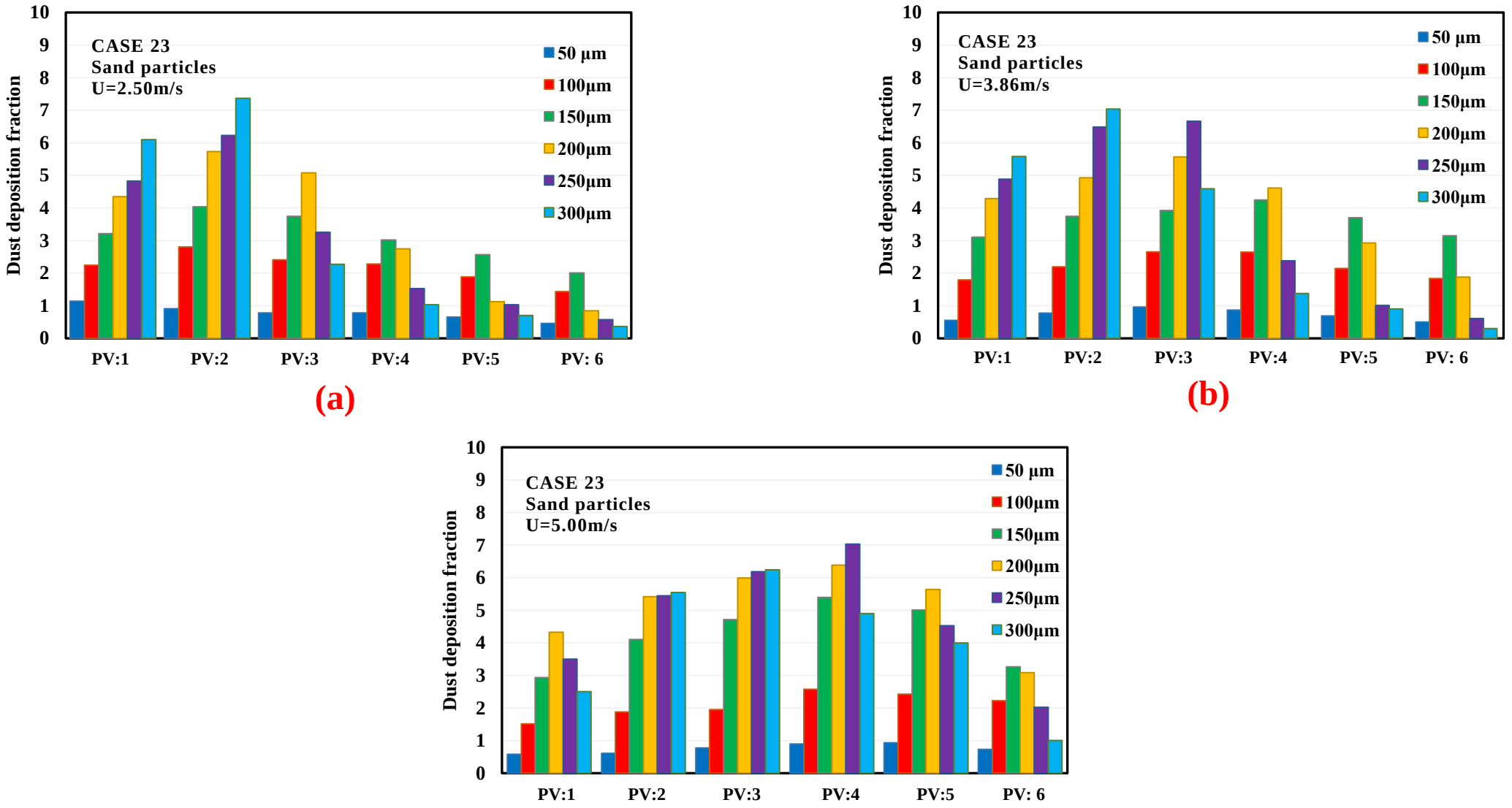

Fig. 9. Dust deposition fractions for different airflow velocities and particle diameters

Predicted efficiency reductions

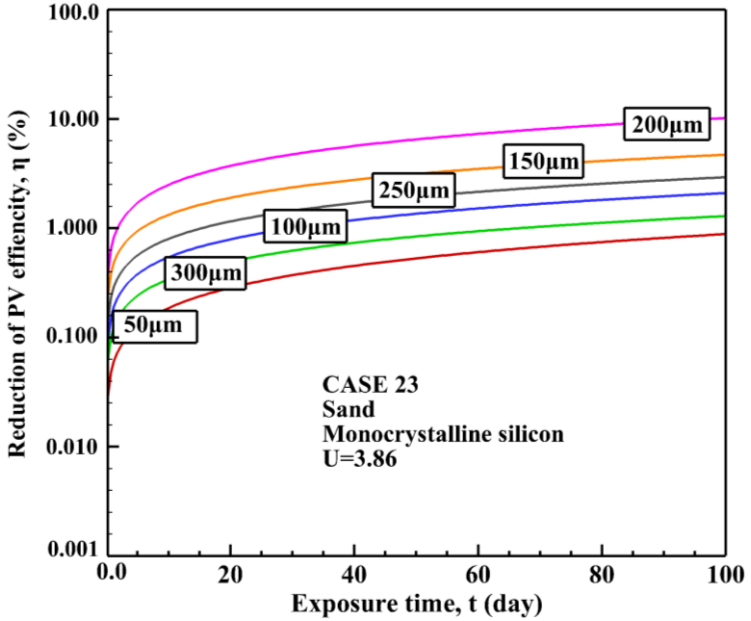

Fig.10(a). Effect of dust deposition on PV module efficiency for different size of particle

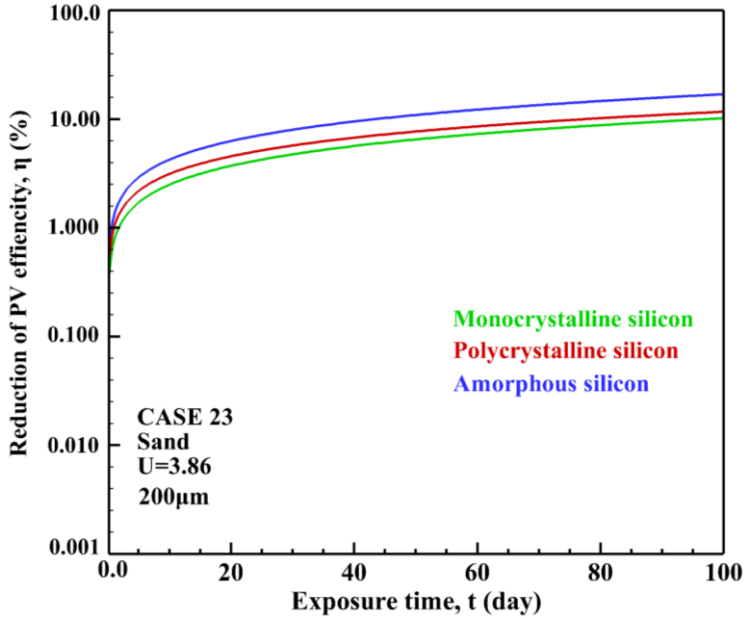

Fig.10(b). Effect of dust deposition on PV module efficiency for different types of PV cells

Efficiency reduction [4]:

$$\eta_{red} = \frac{E_{red}}{E_{clean}} = \kappa \cdot \rho_{dep} =$$

$$\kappa \frac{N_d}{t_d} \frac{m_p}{S_d} T = \kappa \frac{\lambda N_p \rho_p \pi d_p^3}{6 t_d S_d} T \times 100\%$$

E_{red}: *PV module efficiency with dust accumolation*
E_{clean}: *PV module efficiency without dust accumolation*
N_p: *Number of released dust particles;*
N_d: *Number of deposited dust particles on PV module*;
t_d: *Time period*;
κ: *Influencing factor of dust density on PV efficiency;*
m_p: *The mass of each dust particle*;
S_d: *The PV panel area*;
T: *Exposure time (day);*
λ: *The dust deposition fraction*;
ρ_p: *Density of particle*;
d_p: *Dust particle diameter*.

[6] Hao Lu, Lin Lu, Yuanhao Wang, Applied Energy, 180 (2016) 27-36.

Conclusions

- **The optimum solid wind barrier directs 95% of dust particles to pass over the PV panels, with less than 5% of dust particles being deposited on the panel surfaces.**

- **The largest dust deposition fraction for the first three PV panels for different wind velocities is for particles diameters in the range of 200 μm ≤ dp ≤ 300 μm.**

- **The minimum PV module efficiency reduction is for the deposition and accumulation of 50 μm dust particles (Smallest size studied).**

- **The minimum PV module efficiency reduction is for monocrystalline cells.**

- **The presented simulation results were in good agreement with earlier CFD and experimental studies reported in the literature.**

Thank You!

Questions